

Received 9 April 2019; revised 13 July 2019; accepted 14 July 2019. Date of publication 25 July 2019;  
date of current version 9 August 2019. The review of this paper was arranged by Editor M. Chan.

Digital Object Identifier 10.1109/JEDS.2019.2931015

# Optimization of $Zn_2SiO_4$ Anode Structure for Deep Ultraviolet Generation With Carbon Nanotube Emitters

SUNG TAE YOO<sup>ID</sup>, HYE IN LEE, AND KYU CHANG PARK<sup>ID</sup>

Department of Information Display, Kyung Hee University, Seoul 02447, South Korea

CORRESPONDING AUTHOR: K. C. PARK (e-mail: kyupark@khu.ac.kr)

This work was supported in part by the Radiation Technology Research and Development Program through the National Research Foundation of Korea (NRF) funded by the Ministry of Science and ICT under Grant NRF-2017M2A2A4A01020658, and in part by the BK21 Plus Program (Future-Oriented Innovative Brain Raising Type) funded by the Ministry of Education, South Korea, and the NRF under Grant 21A20130000018.

**ABSTRACT** Ultraviolet (UV) light is applied to various industrial and medical devices. In particular, deep UV light with short wavelengths could minimize the damage to human cells when it is used to virus and bacterial sterilization. We optimized the  $Zn_2SiO_4$  anode structure to improve deep UV light generation with a carbon nanotube (CNT) cold cathode based electron beam (C-beam) pumping. Annealing at 1000 °C and 400 mTorr produces anode with the highest deep UV intensity. Using a 100-nm  $SiO_x$  layer between  $Zn_2SiO_4$  and quartz substrate, the intensity of deep UV light at a wavelength of 226 nm was increased by 1.8 times.

**INDEX TERMS** Deep ultraviolet,  $Zn_2SiO_4$ , carbon nanotube, electron emission.

## I. INTRODUCTION

Deep ultraviolet (UV) has high photon energy and could be applied in many applications such as disinfection, odor removal, optical cleaning and medical uses. UV disinfection technology is essential for safe water and air, which is basic needs of human life. Deep UV light with short wavelengths can mitigate damage to human cells during virus and bacterial sterilization because short wavelengths can reduce mutagenic and cytotoxicity damage to human cells [1]–[3].

Currently, mercury vapor lamps are mostly used as light sources for UV disinfection. As mercury regulations are progressing in response to increasing environmental demands, research on light-emitting diodes (LEDs) is underway [4], [5]. LEDs are widely used in visible and UV applications, but there are many problems to be utilized in deep UV region [5]–[11]. The main problem is low efficiency due to the deep UV absorption and potential of AlGaN owing to the mismatch in epitaxial layer and the substrate [6]–[11]. In addition, it is difficult to make large area UV LEDs because of the leakage current in junction and point light source. Various studies have been done to overcome these issues, and one of the alternative

technologies is deep UV generation using electron beam pumping technology [12]–[16].

Carbon nanotube (CNT) emitters are the most appropriate cold cathode electron sources for electron beam pumping technology due to their outstanding electrical, chemical and mechanical characteristics [17]. Based on the excellent properties of CNT emitters, they are being studied for electron devices such as field emission lamps, X-ray tubes, and electron microscopes [18]–[21]. In particular, CNT emitters are capable of generating UV light in large areas, thus demonstrating their advantages as an electronic source for UV generation. We had grown fully vertical aligned CNT emitters with homemade direct current plasma enhanced chemical vapor deposition (DC-PECVD) [22] and used it as an excitation source to generate deep UV light. We called the CNT cold cathode based electron beam “C-beam.”

Deep UV generation using electron beam pumping technology depends on the properties of the anode materials. Wide bandgap materials such as hexagonal boron nitride (h-BN), aluminum nitride-based quantum wells,  $ZnAl_2O_4$ , and  $Zn_2SiO_4$  are being studied as anode materials for UV generation [13]–[16]. Watanabe and colleagues made deep

UV with a wavelength of 225 nm using h-BN [13]. As reported by Oto *et al.*, aluminum nitride based quantum wells were used as an anode material to make a wavelength of 240 nm [14]. Ishinaga *et al.* controlled the composition ratio of  $ZnAl_2O_4$  to obtain deep UV emission peak of 250 to 270 nm [15]. We obtained deep UV with wavelengths of 208, 226 and 244 nm using  $Zn_2SiO_4$  and C-beam pumping technology [16].

Recently, research is being conducted to improve the light intensity of electron devices using silicon element. Cheng *et al.* have improved the blue light electroluminescent power of LEDs from 0.1 to 0.7  $\mu\text{W}$  by changing the size of the silicon quantum dots [23]. Si-LEDs have improved the device performance by increasing the electric field confinement and high speed response through the avalanche mode [24], [25]. In this study, we fabricated  $Zn_2SiO_4$  by diffusing the silicon element of the  $\text{SiO}_x$  layer into the  $\text{ZnO}$  layer using thermal energy in the furnace, and improved the deep UV characteristics at 226 nm by C-beam irradiation. With the  $\text{SiO}_x$  layer, the UV light intensity at 226 nm was 1.8 times higher than that of conventional structure without  $\text{SiO}_x$  layer.

## II. EXPERIMENT DETAILS

Fig. 1 shows the schematic diagram of deep UV generation with C-beam pumping. The anode has a quartz substrate, UV-C layer, and an aluminum (Al) electrode. We used a quartz substrate with a length of 40 mm and a width of 20 mm. The UV-C layer contains  $Zn_2SiO_4$  as a layer for generating deep UV by electron beam irradiation. The  $Zn_2SiO_4$  was fabricated by spin-coating and annealing  $\text{ZnO}$  ink solution on a quartz substrate. Zinc acetate dihydrate (ZAD), monoethanolamine, and 2-methoxyethanol were stirred at 70 °C for 5 hours to prepare a  $\text{ZnO}$  ink solution [26]. The ZAD concentration of the  $\text{ZnO}$  ink solution is 0.3 mol. In the annealing process, nitrogen ( $N_2$ ) gas was injected into the furnace and the process was performed at 1,000 °C for 1 hour.  $Zn_2SiO_4$  was formed after the annealing process and Al electrode was deposited with the Al thermal evaporation technique to form an anode electrode [16]. In order to improve the deep UV light intensity,  $\text{SiO}_x$  and  $\text{SiN}_x$  were deposited on the quartz with a thickness of 100 nm using PECVD.

We used the C-beam of triode structure to generate deep UV. The triode structure consisted of a cathode, gate, and anode as shown in Fig. 1(a). The cathode had CNT emitters. The fabrication process of the CNT emitters is shown in Fig. 2 [27]–[29]. The Si wafer with a size of 15 x 15 mm<sup>2</sup> was used as a substrate for manufacturing CNT emitters. The deposition of the nickel catalyst on the Si wafer was used for sputtering as shown in Fig. 2 (a). The thickness of Ni is 20 nm. Fig. 2(b) shows photoresist spin coating and patterning through photolithography. In order to fabricate CNT emitters at desired locations, photoresist was patterned in the form of a dot having a diameter of 3  $\mu\text{m}$  on the Ni layer. After photolithography, we proceeded to Ni etching,

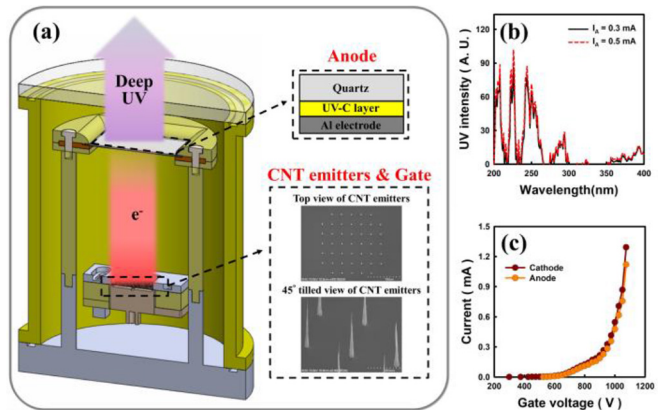


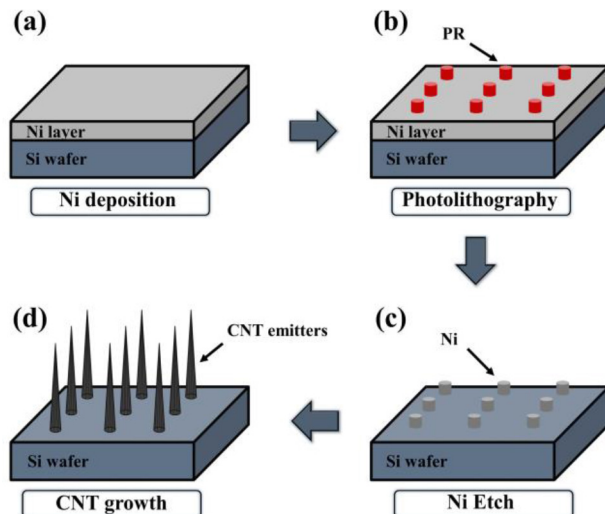
**FIGURE 1.** Deep-UV generation with a carbon nanotube cold cathode based electron beam: (a) a schematic diagram of deep UV generation [Inset: cross-sectional view of anode structure (top) and the SEM image of CNT emitters (bottom)]. (b) the UV spectra with CNT cold cathode electron beam irradiation. (c) electron emission characteristics of CNT emitters.

which is the etching of the Ni layer, as shown in Fig. 2 (c). The Ni catalyst was selectively patterned on Si wafer using photolithography and Ni etching. Fig. 2 (d) shows the schematic image of grown CNT emitters by homemade DC-PECVD. The shape of the grown CNT emitters is shown the SEM image inset in Fig. 1(a). The CNT emitters have dot size of 3  $\mu\text{m}$  and height of about 40  $\mu\text{m}$  and they are vertically and conically grown. Each CNT emitters is patterned at 30  $\mu\text{m}$  intervals to reduce field screening between CNT emitters. The gate electrode was used for electron extraction [27]. Ceramic was used for insulation between the cathode and the gate. We kept the distance between the cathode and the gate at 250  $\mu\text{m}$ . The electron emission characteristics of the CNT emitters are shown in the Fig. 1(c). At an anode voltage ( $V_a$ ) of 7 kV and a gate voltage of 1,075 V, an anode current ( $I_a$ ) is 1.12 mA and the electron transmission rate through the gate hole is 86.6%. When the  $I_a$  is more than 0.3 mA, deep UV is generated as shown in the Fig. 1(b). The UV peak positions do not change with  $I_a$  and were observed at wavelengths of 208, 226, and 244 nm. In the previous study, the origin of deep UV with peaks at wavelengths of 208, 226, and 244 nm is rhombohedral  $Zn_2SiO_4$  [16], [30].

To evaluate the characteristics of deep UV light, Avaspec-ULS2048 UV spectrometer of Avantes was used. The morphology of  $Zn_2SiO_4$  film were confirmed using a scanning electron microscope (SEM, Hitachi S-4700). To determine the material of the UV-C layer, Empyrean X-ray diffraction (XRD) system from PANalytical was used. Agilent 34401A, Keithley 248, and Spellman ST system were used as power supply and to measure current.

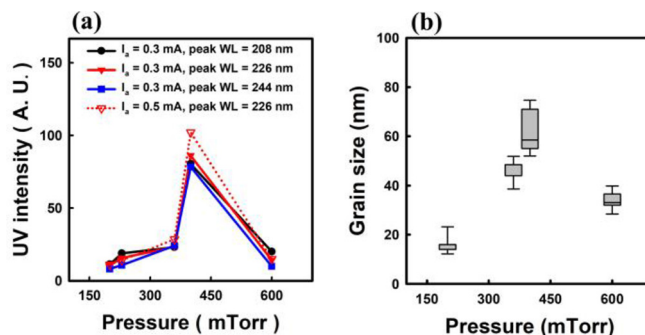
## III. RESULTS AND DISCUSSION

Fig. 3 shows the UV intensities and grain sizes of the  $Zn_2SiO_4$  anode with various annealing pressures at 1,000 °C. Deep UV intensities depend on the pressure in the furnace. Fig. 3(a) shows the UV intensities of the anode annealed with various pressure at the  $I_a$  of 0.3 mA and



**FIGURE 2.** The fabrication process of the CNT emitters: (a) Deposition of nickel on the Si wafer with sputtering. (b) Photolithograph for the selectively patterning. (c) Etching of nickel catalyst layer. (d) Growth of CNT emitters with DC-PECVD.

0.5 mA. The UV intensity is the highest at pressure of 400 mTorr, regardless of the three peak wavelengths of 208, 226 and 244 nm. The trend of grain size variation with pressure overlaps well with UV intensity variation. At pressure of 400 mTorr, the grain size of UV-C layer is the largest at 60 nm and the UV intensity is the highest. As shown in Fig. 3(a), at the  $I_a$  of 0.3 mA, the UV intensity at 226 nm of the 400 mTorr annealed sample exhibits 8.1 times greater than 200 mTorr one. It exhibits the lowest UV intensity at 200 mTorr regardless of wavelength and has the smallest grain size. Also, the observed UV peak positions at 208, 226, and 244 nm did not change with  $I_a$  of 0.5 mA. At a wavelength of 226 nm, the UV intensity of the sample at  $I_a$  of 0.5 mA is 1.2 times greater than that of the 0.3 mA.



**FIGURE 3.** (a) The UV intensities and (b) grain size variation of the anode annealed with various pressure.

$SiO_x$  and  $SiN_x$  were used between the quartz substrate and the  $Zn_2SiO_4$  thin film to increase the deep UV intensity. Fig. 4 shows various anode structures before annealing process and UV spectra depending on the anode structures. The anode structure of Fig. 4(a) is a conventional structure, which is a ZnO ink solution spin-coated onto a quartz

substrate. In the case of Fig. 4(b) and (c),  $SiO_x$  and  $SiN_x$  films were deposited on quartz substrate with a thickness of 100 nm and then the ZnO ink solution was spin-coated on the films. For structural modification, annealing was carried out at 1000 °C for 1 hour after injection of  $N_2$  gas and maintaining a pressure of 400 mTorr. After annealing, we obtained  $Zn_2SiO_4$  anode film. Fig. 4(d) shows the deep UV spectra obtained with C-beam pumping with  $V_a$  of 7 kV and  $I_a$  of 0.3 mA. The UV spectra depend on the films used on the quartz substrate. When we used the  $SiO_x$  layer, a deep UV of 226, 244 nm wavelength was obtained. The UV intensity at a wavelength of 208 nm is lower than without the  $SiO_x$  layer. However, at 226 and 244 nm, the deep UV intensities were increased by 1.8 and 1.5 times, respectively, compared to the conventional structure of Fig. 4(a). When 100 nm  $SiN_x$  was used, the peak wavelength was observed at 308 nm, but the intensity was weak. In addition, UV light of wavelengths of 250 nm or less disappeared. This is related to the bandgap energy. The bandgap energies of crystalline silicon nitride ( $Si_3N_4$ ) and silicon dioxide ( $SiO_2$ ) are  $\sim 5$  eV and  $\sim 9$  eV, respectively. Using  $SiN_x$ , the generated deep UV is absorbed by  $Si_3N_4$  existing in  $SiN_x$  because the band gap energy is smaller than that of  $Zn_2SiO_4$ . However, in the case of  $SiO_x$  layer, the band gap energy is larger than that of  $Zn_2SiO_4$ , so deep UV is not absorbed.

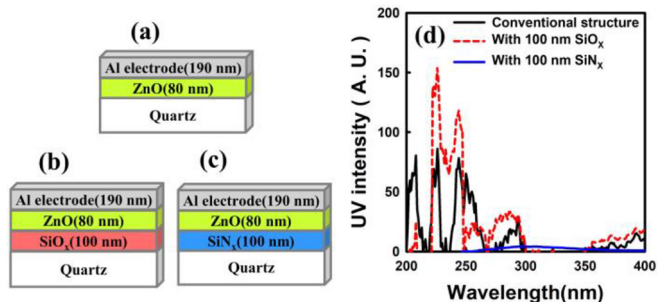


**FIGURE 4.** UV performance with variable anode structure: (a) conventional structure, (b) with 100 nm  $SiO_x$  and, (c) with 100 nm  $SiN_x$ . (a), (b) and (c) are structures before annealing at 1000 °C. (d) The UV spectra with various anode structures after annealing process.

To understand the enhanced deep UV light intensity, variable  $Zn_2SiO_4$  anode structures were measured with SEM. Fig. 5 shows a SEM image of  $Zn_2SiO_4$  anodes with various structures after the annealing process. In the case of the conventional structure, certain grains are easily visible, and their size is about 60 nm as shown in Fig. 5(a). Fig. 5(b) shows SEM image of  $Zn_2SiO_4$  on 100 nm  $SiO_x$  after annealing. The grains are formed in various shapes rather than circular shapes and the size of grains is larger than 100 nm. The largest grains of 100 nm or more were observed and the grains were well connected. When 100 nm  $SiN_x$  was used, grains of various sizes ranging from 26 nm to 169 nm were formed. However, the grains were not connected and were non-uniform.

In Fig. 3, the UV intensities are changed based on the tendency of change in grain size. This tendency can also be

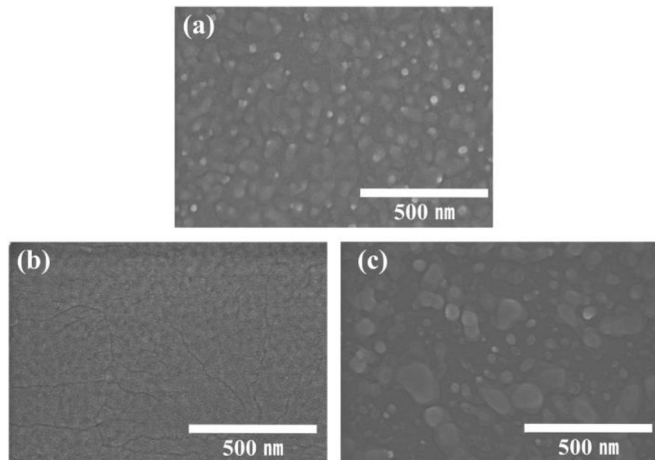


**FIGURE 5.** The SEM images after annealing with various anode structures: (a) conventional structure, (b) with 100 nm SiO<sub>x</sub>, and (c) 100 nm SiN<sub>x</sub> on quartz substrate.

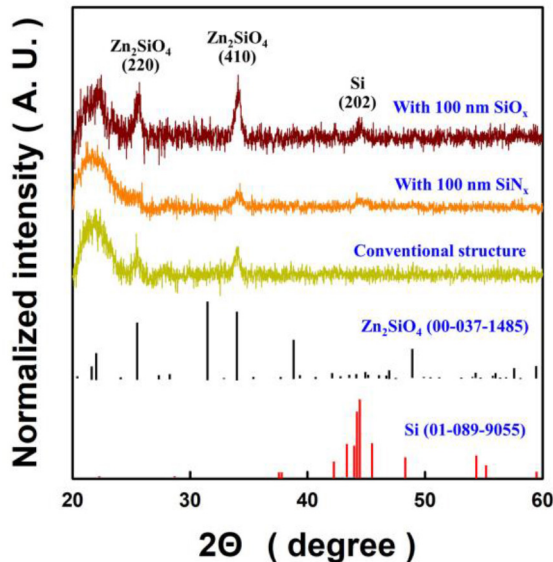


**FIGURE 6.** XRD results with different anode structure after annealing process.

seen in UV intensity variation according to different anode structures. When SiO<sub>x</sub> layer was used, it had the highest intensity at 226 nm wavelength and the largest grain size of 100 nm or more. Increased UV intensities and grain size are associated with the amorphous structure of the SiO<sub>x</sub> and SiN<sub>x</sub>. In order to form Zn<sub>2</sub>SiO<sub>4</sub> film, silicon of the quartz substrate should be supplied to the ZnO layer during the annealing process. The quartz substrate is crystalline structure and structural modification is difficult to supply for the silicon element. On the other hand, the amorphous structure of the SiO<sub>x</sub> and SiN<sub>x</sub> is more easily structurally modified to feed the silicon element onto the ZnO. When SiN<sub>x</sub> is used, SiN<sub>x</sub> acts as a barrier to Zn diffusion, so the grains are not uniform and the UV intensity is low [31].

To apprehend origin of enhanced grain size of Zn<sub>2</sub>SiO<sub>4</sub> on SiO<sub>x</sub> layer, we performed XRD analysis. Fig. 6 shows XRD results with different anode structure after annealing process. Regardless of the anode structure, a broad peak from quartz substrate was observed at around 22.3°. The 25.5° and 34.0° peaks were attributed to the (220) and (410) planes (rhombohedral zinc silicate, JCPDS card number 00-037-1485). The (220) and (410) planes Zn<sub>2</sub>SiO<sub>4</sub> peaks enhanced with 100 nm SiO<sub>x</sub> anode. This result is presumed to be related to increase the intensity of the wavelengths of 226, 244 nm using SiO<sub>x</sub>. When SiO<sub>x</sub> and SiN<sub>x</sub> were used, unlike the conventional structure, a peak was detected at 44.3° which is the peak of the (202) plane of Si (orthorhombic silicon, JCPDS card number 01-089-9055). The Si related peaks are expected to be caused by diffusion of Si during the annealing process, and this result is also considered to have affected the UV characteristics. However, the relationship between crystalline plane of Zn<sub>2</sub>SiO<sub>4</sub> and respective UV peaks of 208, 226 and 244 nm is not clear and needs more study.

#### IV. CONCLUSION

In summary, we optimized the Zn<sub>2</sub>SiO<sub>4</sub> anode structure to improve 226 nm deep UV light generation with carbon nanotube emitters. Wide bandgap SiO<sub>x</sub> layer between anode and substrate was used to enhance deep UV generation. The intensity of the deep UV was related to grain size and uniformity of Zn<sub>2</sub>SiO<sub>4</sub>. The grain size of Zn<sub>2</sub>SiO<sub>4</sub> increased from 60 nm to larger than 100 nm with inserting deposited SiO<sub>x</sub> on quartz substrate. Deep UV light intensity at a peak wavelength at 226 nm increased by 1.8 times than without SiO<sub>x</sub> layer. This deep UV enhancement is due to the better diffusion of the Si element into the ZnO layer when using the SiO<sub>x</sub> layer than the conventional structure.

#### REFERENCES

- [1] M. Buonanno *et al.*, “207-nm UV light—A promising tool for safe low-cost reduction of surgical site infections. I: In vitro studies,” *PLoS ONE*, vol. 8, no. 10, Oct. 2013, Art. no. e76968. doi: [10.1371/journal.pone.0076968](https://doi.org/10.1371/journal.pone.0076968).
- [2] D. Welch *et al.*, “Far-UVC light: A new tool to control the spread of airborne-mediated microbial diseases,” *Sci. Rep.*, vol. 8, no. 1, Feb. 2018, Art. no. 2752. doi: [10.1038/s41598-018-21058-w](https://doi.org/10.1038/s41598-018-21058-w).
- [3] S. E. Beck, R. A. Rodriguez, K. G. Linden, T. M. Hargy, T. C. Larason, and H. B. Wright, “Wavelength dependent UV inactivation and DNA damage of adenovirus as measured by cell culture infectivity and long range quantitative PCR,” *Environ. Sci. Technol.*, vol. 48, no. 1, pp. 591–598, Dec. 2013. doi: [10.1021/es403850b](https://doi.org/10.1021/es403850b).
- [4] H. Hirayama, N. Maeda, S. Fujikawa, S. Toyoda, and N. Kamata, “Recent progress and future prospects of AlGaN-based high-efficiency deep-ultraviolet light-emitting diodes,” *Jpn. J. Appl. Phys.*, vol. 53, no. 10, Sep. 2014, Art. no. 100209. doi: [10.7567/JJAP.53.100209](https://doi.org/10.7567/JJAP.53.100209).
- [5] J. Chen, S. Loeb, and J.-H. Kim, “LED revolution: Fundamentals and prospects for UV disinfection applications,” *Environ. Sci. Water Res.*, vol. 3, no. 2, pp. 188–202, 2017. doi: [10.1039/c6ew00241b](https://doi.org/10.1039/c6ew00241b).
- [6] N. Maeda and H. Hirayama, “Realization of high-efficiency deep-UV LEDs using transparent p-AlGaN contact layer,” *Physica Status Solidi C*, vol. 10, no. 11, pp. 1521–1524, Oct. 2013. doi: [10.1002/pssc.201300278](https://doi.org/10.1002/pssc.201300278).
- [7] T. Takano, T. Mino, J. Sakai, N. Noguchi, K. Tsubaki, and H. Hirayama, “Deep-ultraviolet light-emitting diodes with external quantum efficiency higher than 20% at 275 nm achieved by improving light-extraction efficiency,” *Appl. Phys. Exp.*, vol. 10, no. 3, Feb. 2017, Art. no. 031002. doi: [10.7567/APEX.10.031002](https://doi.org/10.7567/APEX.10.031002).

- [8] N. Maeda, J. Yun, M. Jo, and H. Hirayama, "Enhancing the light-extraction efficiency of AlGaN deep-ultraviolet light-emitting diodes using highly reflective Ni/Mg and Rh as p-type electrodes," *Jpn. J. Appl. Phys.*, vol. 57, no. 4S, Mar. 2018, Art. no. 04FH08. doi: [10.7567/JJAP.57.04FH08](https://doi.org/10.7567/JJAP.57.04FH08).
- [9] K. Xu *et al.*, "Light emission from a poly-silicon device with carrier injection engineering," *Mater. Sci. Eng. B*, vol. 231, pp. 28–31, May 2018. doi: [10.1016/j.mseb.2018.07.002](https://doi.org/10.1016/j.mseb.2018.07.002).
- [10] B. Viana, O. Lupon, and T. Pauporté, "Directional and magnetic field enhanced emission of Cu-doped ZnO nanowires/p-GaN heterojunction light-emitting diodes," *J. Nanophoton.*, vol. 5, no. 1, Jan. 2011, Art. no. 051816. doi: [10.1117/1.3604783](https://doi.org/10.1117/1.3604783).
- [11] S. Nakamura, "The roles of structural imperfections in InGaN-based blue light-emitting diodes and laser diodes," *Science*, vol. 281, no. 5379, pp. 956–961, Aug. 1998. doi: [10.1126/science.281.5379.956](https://doi.org/10.1126/science.281.5379.956).
- [12] D. Li, K. Jiang, X. Sun, and C. Guo, "AlGaN photonics: Recent advances in materials and ultraviolet devices," *Adv. Opt. Photon.*, vol. 10, no. 1, pp. 43–110, Jan. 2018. doi: [10.1364/AOP.10.000043](https://doi.org/10.1364/AOP.10.000043).
- [13] K. Watanabe, T. Taniguchi, T. Niizuma, K. Miya, and M. Taniguchi, "Far-ultraviolet plane-emission handheld device based on hexagonal boron nitride," *Nat. Photon.*, vol. 3, no. 10, pp. 591–594, Sep. 2009. doi: [10.1038/nphoton.2009.167](https://doi.org/10.1038/nphoton.2009.167).
- [14] T. Oto, R. G. Banal, K. Kataoka, M. Funato, and Y. Kawakami, "100 mW deep-ultraviolet emission from aluminium-nitride-based quantum wells pumped by an electron beam," *Nat. Photon.*, vol. 4, no. 11, pp. 767–770, Sep. 2010. doi: [10.1038/nphoton.2010.220](https://doi.org/10.1038/nphoton.2010.220).
- [15] T. Ishinaga, T. Iguchi, H. Kominami, K. Hara, M. Kitaura, and A. Ohnishi, "Luminescent property and mechanism of ZnAl<sub>2</sub>O<sub>4</sub> ultraviolet emitting phosphor," *Physica Status Solidi C*, vol. 12, no. 6, pp. 797–800, May 2015. doi: [10.1002/pssc.201400317](https://doi.org/10.1002/pssc.201400317).
- [16] S. T. Yoo, J. H. Hong, J. S. Kang, and K. C. Park, "Deep-ultraviolet light source with carbon nanotube cold-cathode electron beam," *J. Vac. Sci. Technol. B*, vol. 36, no. 2, Mar. 2018, Art. no. 02C103. doi: [10.1116/1.5004621](https://doi.org/10.1116/1.5004621).
- [17] M. F. L. De Volder, S. H. Tawfick, R. H. Baughman, and A. J. Hart, "Carbon nanotubes: Present and future commercial applications," *Science*, vol. 339, no. 6119, pp. 535–539, Jan. 2013. doi: [10.1126/science.1222453](https://doi.org/10.1126/science.1222453).
- [18] N. Ichikawa, K. Ikeda, Y. Honda, H. Taketomi, K. Kawai, and T. Suzuki, "Development of a UV light source using Pr: LuAG thin film pumped by electron beam," *Elect. Commun. Jpn.*, vol. 99, no. 10, pp. 33–39, Sep. 2016. doi: [10.1002/ecj.11870](https://doi.org/10.1002/ecj.11870).
- [19] K. Morishita, K. Fujita, R. Kakei, H. Furuki, and T. Okada, "Carbon nanotube sheets used in field-emission lamps with vacuum-sealed diode structures," *Fullerenes Nanotubes Carbon Nanostruct.*, vol. 24, no. 5, pp. 293–297, Mar. 2016. doi: [10.1080/1536383X.2016.1154048](https://doi.org/10.1080/1536383X.2016.1154048).
- [20] J. H. Hong, J. S. Kang, and K. C. Park, "Fabrication of a compact glass-sealed X-ray tube with carbon nanotube cold cathode for high-resolution imaging," *J. Vac. Sci. Technol. B*, vol. 36, no. 2, Mar. 2018, Art. no. 02C109. doi: [10.1116/1.5007106](https://doi.org/10.1116/1.5007106).
- [21] H. R. Lee, H. H. Yang, and K. C. Park, "Fabrication of a high-resolution electron beam with a carbon nanotube cold-cathode," *J. Vac. Sci. Technol. B*, vol. 35, no. 6, Nov. 2017, Art. no. 06G804. doi: [10.1116/1.4991920](https://doi.org/10.1116/1.4991920).
- [22] S. H. Lim *et al.*, "Controlled density of vertically aligned carbon nanotubes in a triode plasma chemical vapor deposition system," *Thin Solid Films*, vol. 515, no. 4, pp. 1380–1384, Dec. 2006. doi: [10.1016/j.tsf.2006.03.056](https://doi.org/10.1016/j.tsf.2006.03.056).
- [23] C.-H. Cheng, Y.-C. Lien, C.-L. Wu, and G.-R. Lin, "Multicolor electroluminescent Si quantum dots embedded in SiO<sub>x</sub> thin film MOSLED with 2.4% external quantum efficiency," *Opt. Exp.*, vol. 21, no. 1, p. 391, Jan. 2013. doi: [10.1364/OE.21.000391](https://doi.org/10.1364/OE.21.000391).
- [24] K. Xu, "Monolithically integrated Si gate-controlled light-emitting device: Science and properties," *J. Opt.*, vol. 20, no. 2, Jan. 2018, Art. no. 024014. doi: [10.1088/2040-8986/aaa2b7](https://doi.org/10.1088/2040-8986/aaa2b7).
- [25] K. Xu, "Silicon MOS optoelectronic micro-nano structure based on reverse-biased PN junction," *Physica Status Solidi A*, vol. 216, no. 7, Apr. 2019, Art. no. 1800868. doi: [10.1002/pssa.201800868](https://doi.org/10.1002/pssa.201800868).
- [26] L. Znaidi, "Sol-gel-deposited ZnO thin films: A review," *Mater. Sci. Eng. B*, vol. 174, nos. 1–3, pp. 18–30, Oct. 2010. doi: [10.1016/j.mseb.2010.07.001](https://doi.org/10.1016/j.mseb.2010.07.001).
- [27] J. S. Kang, J. H. Hong, and K. C. Park, "High-performance carbon-nanotube-based cold cathode electron beam with low-thermal-expansion gate electrode," *J. Vac. Sci. Technol. B*, vol. 36, no. 2, Mar. 2018, Art. no. 02C104. doi: [10.1116/1.5005025](https://doi.org/10.1116/1.5005025).
- [28] K. C. Park, J. H. Ryu, K. S. Kim, Y. Y. Yu, and J. Jang, "Growth of carbon nanotubes with resist-assisted patterning process," *J. Vac. Sci. Technol. B*, vol. 25, no. 4, p. 1261, 2007. doi: [10.1116/1.2752513](https://doi.org/10.1116/1.2752513).
- [29] J. H. Ryu, N. Y. Bae, H. M. Oh, O. Zhou, J. Jang, and K. C. Park, "Stabilized electron emission from silicon coated carbon nanotubes for a high-performance electron source," *J. Vac. Sci. Technol. B*, vol. 29, no. 2, Mar. 2011, Art. no. 02B120. doi: [10.1116/1.3565428](https://doi.org/10.1116/1.3565428).
- [30] S. Z. Karazhanov, P. Ravindran, H. Fjellvåg, and B. G. Svensson, "Electronic structure and optical properties of ZnSiO<sub>3</sub> and Zn<sub>2</sub>SiO<sub>4</sub>," *J. Appl. Phys.*, vol. 106, no. 12, Dec. 2009, Art. no. 123701. doi: [10.1063/1.3268445](https://doi.org/10.1063/1.3268445).
- [31] W. X. Zou, G. A. Vawter, J. L. Merz, and L. A. Coldren, "Behavior of SiN<sub>x</sub> films as masks for Zn diffusion," *J. Appl. Phys.*, vol. 62, no. 3, pp. 828–831, Aug. 1987. doi: [10.1063/1.339714](https://doi.org/10.1063/1.339714).



**SUNG TAE YOO** received the B.S. degree in mechanical engineering from Chungbuk National University, South Korea, in 2013, and the M.S. degree from the Department of Information Display, Kyung Hee University, South Korea, in 2017, where he is currently pursuing the Ph.D. degree. His technical interests are in the field emission, carbon nanotube, and electron beam pumped light source.



**HYE IN LEE** received the B.S. degree from Sangji University, South Korea, in 2017. She is currently pursuing the M.S. degree with Kyung Hee University, South Korea. Her current research interest includes the deep ultraviolet with carbon nanotube electron beam.



**KYU CHANG PARK** received the Ph.D. degree in semiconductor physics from the Department of Physics, Kyung Hee University, South Korea, in 1997. He was with Hyundai Electronics Inc. (Currently, Hynix Semiconductor, Inc.) from January 1997 to August 2002. Since September 2002, he has been a Professor with the Department of Information Display, Kyung Hee University. He has published many papers on fabrication of cold cathode electron beam with carbon nanotube electron sources and its application to display, lighting, X-ray devices and thin-film crystallization. His current research interest is the fabrication of high performance electron sources, deep ultraviolet, X-ray tubes and multi X-ray beam for tomo-synthesis, electron microscope, and multibeam electron lithography techniques with carbon nanotube cold cathode electron beam.